Published in final edited form as:
Nanomedicine (Lond). 2010 April ; 5(3): 379–396. doi:10.2217/nnm.10.7.

Macrophage Delivery of Therapeutic Nanozymes in a Murine Model of Parkinson's Disease

Anna M. Brynskikh[1,4], **Yuling Zhao**[1,2], **R. Lee Mosley**[1,3,4], **Shu Li**[1,2], **Michael D. Boska**[1,3,5], **Natalia L. Klyachko**[6], **Alexander V. Kabanov**[1,2,3,4,6], **Howard E. Gendelman**[1,2,3,4], and **Elena V. Batrakova**[1,2,*]

[1]Center for Drug Delivery and Nanomedicine, University of Nebraska Medical Center, Omaha, NE

[2]Department of Pharmaceutical Sciences, University of Nebraska Medical Center, Omaha, NE

[3]Center for Neurodegenerative Disorders, University of Nebraska Medical Center, Omaha, NE

[4]Department of Pharmacology and Experimental Neuroscience, University of Nebraska Medical Center, Omaha, NE

[5]Department of Radiology, University of Nebraska Medical Center, Omaha, NE

[6]Deparment of Chemistry, M.V. Lomonosov State University, Moscow, Russia

Abstract

Background—Parkinson's disease (PD) is a common progressive neurodegenerative disorder associated with profound nigrostriatal degeneration. Regrettably, no therapies are currently available that can attenuate disease progression. To this end, we developed a cell-based nanoformulation delivery system using the antioxidant enzyme, catalase, to attenuate neuroinflammatory processes linked to neuronal death.

Methods—Nanoformulated catalase was obtained by coupling catalase to a synthetic polyelectrolyte of opposite charge leading to the formation of a polyion complex micelle. The nanozyme was loaded into bone marrow macrophages (BMM) and its transport to the substantia nigra pars compacts evaluated in 1-methyl-4-phenyl-1,2,3,6-tetrahydropyridine (MPTP) intoxicated mice.

Results—Therapeutic efficacy of BMM loaded with nanozyme was confirmed by two -fold reductions in micro- gliosis as measured by CD11b expression. A two-fold increase in tyrosine hydroxylase (TH)-expressing dopaminergic neurons was detected in nanozyme-treated compared to untreated MPTP-intoxicated mice. Neuronal survival was confirmed by magnetic resonance spectroscopic imaging. BMM loaded catalase showed sustained release of the enzyme in plasma.

Conclusion—These data support the importance of macrophage-based nanozyme carriage for PD therapies.

Keywords

cell-mediated drug delivery; neuroinflammation; catalase; Parkinson's disease; blood-brain barrier

Successful delivery of therapeutic macromolecules (peptides, proteins, and nucleic acids) to sites of active disease is of primary importance towards improving pharmaceutic efficacy. This

*Correspondence: Elena V. Batrakova, Center for Drug Delivery and Nanomedicine, 985830 Nebraska Medical Center, Omaha, NE 68198-5830; Tel: (402) 559-9364; Fax (402) 559-9365, ebatrako@unmc.edu.

is particularly true for neurodegenerative disorders where therapies are limited [1]. One potential therapeutic target for neurodegenerative diseases is neuroinflammation that is linked, in large measure, to neuronal injury and loss. For Parkinson's disease (PD), targeted delivery of anti-inflammatory and antioxidant medicines to the substantia nigra pars compacta (SNpc) can potentially attenuate neuroinflammation and increase neuronal survival [2]. A significant barrier in realizing such therapeutic modalities is the blood brain barrier (BBB) that is impermeable to a spectrum of macromolecules and proteins. However, a means to penetrate the BBB is through cell-based delivery of proteins or drugs. Mononuclear phagocytes (MP; monocyte, tissue macrophage and microglia), residing within the reticuloendothelial (RES) system, in particular, can potentially bypass BBB limitations as well as protect drug-conjugates from the drug-metabolizing processes of the liver [3,4]. Nonetheless, such technologies remain only in development and as of now conjugated drug formulations have not been clinically realized [5].

Recent works performed in our laboratories sought to develop a novel targeted delivery system using MPs for delivery of antioxidant enzymes across the BBB. The target in particular was the site of neuroinflammation and tested in the 1-methyl-4-phenyl-1,2,3,6-tetrahydropyridine (MPTP) mouse model of PD [6]. The strategy seeks to attenuate the neuroinflammatory processes operative during disease that is closely linked to neurodegeneration. MPs are attractive drug carriers, as they rapidly engulf nanoformulations and migrate to sites of inflammation. As such MPs are capable of disease-site specific drug delivery [7]. Therapeutic modalities delivered in this fashion can include anti-inflammatory agents, such as redox enzymes. Importantly, inflammation in the brain is characterized by extensive MP migration primarily between adjacent endothelial cells through the junctional complexes [7,8] and through cell diapedesis and chemataxis [9]. Furthermore, the functional arsenal of pro-inflammatory myeloid cell carriers consists of endocytosing foreign particles, producing regulatory and tissue re-modeling compounds, and liberating substances stored in intracellular vesicles via exocytosis. These features make it possible to exploit inflammatory cells as a carrier system for targeted delivery of redox-enzymes [10–13].

We previously demonstrated that bone marrow macrophages (BMM) can carry significant amounts of catalase, and then slowly releases the active enzyme over 5–7 days [6]. To preclude BMM-mediated enzyme degradation, catalase was packaged into a block ionomer complex producing particles of nanoscale size, "nanozymes." The enzyme released upon stimulation of nanozyme-ladened BMM decomposed microglial hydrogen peroxide produced upon microglia activation by nitrated alpha-synuclein (N-α-syn) or tumor necrosis factor alpha (TNF-α). Finally, significant amounts of catalase were found localized in brains of mice after transfer of nanozyme-ladened BMM following MPTP intoxication. The present study supports the feasibility of cell-mediated drug delivery to the brain by examining i) the nanozyme loading capacity for cell carriers; ii) the effect of nanozymes on cell viability and function; and iii) the neuroprotective activities of BMM-carried nanozyme against MPTP intoxication. Taken together, the data demonstrate that cell-mediated delivery affords a novel approach for PD therapeutics that can be supported by laboratory and animal models of human disease.

Materials & Methods

Reagents

MPTP, polyethylenimine (PEI) (2K, branched, 50% aq. solution), sulforhodamine-B (SRB), sodium dodecylsulfate (SDS), Sephadex G-25, and Triton X-100 were purchased from Sigma-Aldrich, St. Louis, MO. Catalase from bovine liver erythrocytes was provided by Calbiochem, San Diego, CA. Methoxypolyethylene glycol epoxy (Me-PEG-epoxy) was purchased from Shearwater Polymer Inc., Huntsville, AL. Alexa Fluor 680 Protein Dye Kit was purchased from Molecular Probes, Eugene, OR.

Catalase nanozymes

Nanozyme was synthesized as described [6]. First, the copolymer (PEI-PEG) was synthesized using a modified procedure [14] by conjugation of PEI and Me-PEG-epoxy. Particularly, Me-PEG-epoxy water solution was added to 5% PEI in water and incubated overnight at RT. To purify from excess PEI (as well as from low molecular weight residuals), conjugates were dialyzed in SpectraPore membrane tube with subsequent precipitation in ether. Second, assembling of nanozyme was achieved by mixing catalase with PEI-PEG that was separately dissolved in phosphate-buffered saline (PBS) at RT. The +/− charge ratio (Z) was calculated by dividing the amount of amino groups of PEI-PEG protonated at pH 7.4 [15] by the total amount of Gln and Asp in catalase.

BMM

Bone marrow cells were extracted from femurs of C57Bl/6 male mice 6–7 weeks of age according to previously published protocols [16] and cultured for 12 days in DMEM medium (Invitrogen, Carlsbad, CA) supplemented with 1,000 U/mL macrophage colony-stimulating factor (MCSF, a generous gift from Pfizer-Wyeth Pharmaceutical, Cambridge, MA). BMM were collected on days 12 – 14 of culture, and incubated with nanozyme solution at 37°C for 2 hours for cell loading. Cells were washed 3 times with ice-cold PBS at 500 × g, re-suspended in PBS at concentration of 5×10^7 cells/ml and stored on ice until use.

Catalase and cell radiolabeling

For pharmacokinetics studies, catalase was labeled with ^{125}I isotope using $Na^{125}I$ (PerkinElmer Life, Boston, MA) with IodoBEADS iodination reagent (Pierce Biotechnology, Rockford, IL). Briefly, a mixture of catalase solution (2 mg/ml) and $Na^{125}I$ (with total activity of 500 μCi) pre-incubated with the IodoBEADS, was incubated for 15 minutes and then purified on Illustra NAP™-10 column (Pharmacia Biotech Inc., Piscataway, NJ) according to manufacturer's directions. Then 3 ml labeled catalase (400 μCi/ml, 2 mg/ml) was supplemented with 1 ml PEI-PEG block copolymer solution (4 mg/ml) to obtain nanozyme (+/− ratio, Z=1) as described [6].

BMM (5×10^7 cells) were resuspended in the iodination material ($Na^{125}I$ with total activity of 500 μCi, pre-incubated with the IodoBEADS) and the mixture was incubated at room temperature for 20 minutes. To remove the free iodine, the cells were washed three times with ice-cold PBS before use. For Image Visualization and Infrared Spectroscopy (IVIS) studies, BMM (4.8×10^7 cells) were re-suspended in 0.5 ml sterile assay buffer. Alexa Fluor 680 protein dye was dissolved in 0.5 ml of sterile assay buffer containing 122 mM NaCl, 25 mM $NaHCO_3$, 10 mM glucose, 3 mM KCl, 1.2 mM $MgSO_4$, 0.4 mM K_2HPO_4, 1.4 mM $CaCl_2$ and 10 mM HEPES, and incubated with BMM over night at 37 °C. Following incubation, cells were washed two times with ice-cold PBS before use. For confocal microscopy studies, BMM were labeled with rhodamine isothiocyanate (RITC) as described [6].

BMM loading and release of labeled nanozyme

For loading, BMM (5×10^6 cells/ml) were incubated for two hours with ^{125}I-labeled or rhodamine-labeled nanozyme (+/− ratio, Z=1) at 37°C, washed with PBS and centrifuged at 400 × g for 5 min. The radioactivity levels of the cells loaded with nanozyme and media were measured on Wizard 3' 1480 γ-counter (PerkinElmer Life, Boston, MA). For release studies, cells were loaded with rhodamine-labeled nanozyme for two hours, washed three times with ice-cold PBS, and incubated with fresh media for various time points. The media was replenished every other day. The levels of fluorescence were measured on a Shimadzu RF5000 fluorescent spectrophotometer. Amount of nanozyme was normalized for protein content and

expressed in μg of enzyme per mg of the protein. The experiment was repeated three times with three different BMM preparations.

BMM adherence and migratory activities

α-4 Integrin is a protein on the surface of immune cells that allows passage into the central nervous system (CNS) [17]. Therefore, the effect of nanozyme loading on α-4 integrin expression by BMM was evaluated by fluorescence activated cell sorting (FACS). BMM were collected and incubated with catalase alone or catalase nanozyme for two hours. After incubation BMM were stained with phycoerythrin (PE)-conjugated anti-CD49d antibodies (catalog number 557420); PE-Cy5-conjugated non-specific antibodies (catalog number 553931) were used as isotype control to assess the level of nonspecific binding. All antibodies were purchased from BD Pharmingen (BD Biosciences, San Jose, CA). Following staining, BMM were fixed in 1% BSA/4% paraformaldehyde (PFA) in PBS and analyzed using LSR2 instrument by BD (BD Biosciences, San Jose, CA) and Diva Version 6.1.2 analysis software. Non-loaded BMM served as a control.

To study the effect of nanozyme loading on BMM adherence and transport, confluent bovine brain microvessel endothelial cell (BMVEC) monolayers were used to reflect BBB function. The tracking of monocytes across such an artificial BBB *in vitro* was developed previously [18]. Confluent primary BMVEC retain many of the morphological and biochemical characteristics of the BBB, such as formation of tight junctions and low pinocytic activity [19]. Therefore, this system was used to closely recapitulate *in vivo* mechanisms of monocyte-macrophage mediated transport of nanozyme across the BBB. For adherence studies, BMVEC were isolated from fresh cow brains by enzymatic digestion and density centrifugation, and grown on 24-well plates until confluent (typically, 12 days) as described [20]. BMM, labeled with Alexa Fluor 680, were loaded with catalase nanozyme for one hour (Z=1), washed, and then added to BMVEC monolayers (6×10^5 cells/well). Non-loaded BMM were used as a control. The monocytes were allowed to adhere for 30 minutes at 37°C. Afterward, supernatants were collected, cells washed twice with PBS, solubilized with Tween ×100, and the amount of Alexa Fluor-labeled BMM was measured using a Shimadzu RF5000 fluorescent spectrophotometer as described [21]. BMM adhesion was expressed as the amount of labeled cells/cm^2.

For migratory activity studies, BMVEC were cultured on 24-well polycarbonate membrane inserts until confluent [20]. Trans-epithelial electrical resistance (TEER) values were recorded as indexes of cell viability and monolayer integrity. Fluorescently labeled BMM were loaded with catalase (1 mg/ml) nanozyme. Non-loaded BMM were used as a control. Following pre-incubation with assay buffer, the solution in the upper chamber of BMVEC monolayers was replaced with the loaded BMM at concentration of 2×10^6 cells/well. Macrophage chemotactic factor-1 (MCP-1) (150 ng/ml, R&D Systems, Minneapolis, MN) was placed into the lower chamber and used as chemoattractant [18]. Following six hours incubation at 37°C in a shaker, the BMVEC inserts were removed, placed in 24-well plates and centrifuged for 10 min at 400 × g to pellet the migrating cells to the plate's bottom chamber. The pelleted cells were lysed with Triton X-100 (1%) and the amount of labeled BMM was measured as described below. All experiments were performed in triplicate.

Animals

Male C57Bl/6 mice (Charles River Laboratories, USA) 8 weeks of age were used in neuroinflammation and neuroprotection evaluation experiments. Balb/c male mice of the same age were used in the *in vivo* IVIS experiments to reduce fluorescence quenching by colored skin and fur. The animals were kept five per cage with an air filter cover under light- (12-hours light/dark cycle) and temperature-controlled (22 ± 1°C) environment. All manipulations with

the animals were performed under a sterilized laminar hood. Food and water were given *ad libitum.* The animals were treated in accordance to the *Principles of Animal Care* outlined by National Institutes of Health and approved by the Institutional Animal Care and Use Committee of the University of Nebraska Medical Center.

Histopathological assays

To evaluate possible toxic effects of nanozyme-loaded BMM *in vivo*, naive C57Bl/6 mice were injected with BMM loaded with nanozyme (5×10^6 cells/mouse/100µl), PEI-PEG block copolymer alone, or PBS (control group) via the tail vein (*i.v.*). Forty-eight hours later animals were sacrificed and brain, liver, spleen, and kidney were dissected; washed in ice-cold PBS; postfixed in 10% phosphate-buffered paraformaldehyde; and paraffin embedded. Pathological evaluation of the organs was performed on 5 µm paraffin sections stained with hematoxylin and eosin (H&E). Apoptag Kit (Millipore, Billerica, MA) was used according to manufacturer's directions.

MPTP intoxication

For MPTP-intoxication, recipient mice were administered 15–18 mg (based on free-base) MPTP/kg body weight delivered in PBS by four intraperitoneal injections; each given every two hours as described [22,23]. Twelve hours after the last MPTP injection, mice were injected *i.v.* with nanozyme alone or BMM loaded with nanozyme (5×10^6 cells/mouse). Two days (for neuroinflammation parameters assessment) or seven days (for neuronal survival assessment) after the last MPTP injection, mice were anesthetized with ketamine/xylazine cocktail, and subjected to transcardial perfusion with ice-cold PBS for 5 minutes following 5 minutes of perfusion with 4% ice-cold paraformaldehyde in PBS.

Pharmacokinetic studies of radioactively-labeled BMM loaded nanozymes

BMM (5×10^6 cells/ml) were loaded with ^{125}I-labeled catalase nanozyme (Z=1) as described above. In a parallel experiment, ^{125}I-labeled BMM were loaded with non-labeled nanozyme (Z=1). C57Bl/6 healthy mice were injected in the tail vein (*i.v.*) with i) ^{125}I-labeled nanozyme alone, or ii) ^{125}I-labeled nanozyme loaded into BMM, or iii) ^{125}I-labeled BMM loaded with non-labeled nanozyme (5×10^6 cells in 100 µl, 4 µCi /mouse). Blood samples (100 µl) at 24, 48, 72, 120 and 168 hours after the injection were taken from facial vein into heparin-coated microhematocrit tubes (Braintree ScientificBraintee, MA), centrifuged for 5 min at 400 × g, and level of radioactivity was recorded in plasma and in the cell pellet. The amount of catalase in plasma or cell fraction was calculated from the following equation:

$$\%\mathrm{Inj/g}=(\mathrm{Cp/Inj})\times 100,$$

where Cp is the level radioactivity measured in plasma or cell pellet obtained from 1 g of whole blood, and Inj is the total CPM injected *i.v.* Five mice were used for each treatment group.

Bioimaging and infrared spectroscopy (IVIS)

To reduce fluorescence quenching by fur, Balb/c mice were shaved and kept on liquid diet for 48 hours prior to intoxication with MPTP. Catalase used for nanozyme preparation and mature monocytes (isolated from Balb/c donor mice) were labeled separately with Alexa Fluor 680 (emission peak of 680) according to manufacturer's instructions. Then, either labeled BMM were loaded with non-labeled nanozyme (1mg/ml catalase, Z = 1) or nanozyme made of labeled catalase and PEI-PEG was loaded to non-labeled mature monocytes. The labeled BMM-nanozymes were administered *i.v.* to MPTP-treated mice (5×10^6/mouse in 100 µl PBS). The control group was injected with labeled catalase nanozyme alone (without cell carriers). All

three solutions were injected at the same levels of fluorescence. For background fluorescence level evaluation, all animals were imaged before the injections in the IVIS 200 Series imaging system (Caliper, Xenogen Co., Life Sciences). Then, animals were imaged at various time points (1–120 hours) post-treatment.

Western Blot Analysis

Western blot technique was applied to determine glial fibrillary acidic protein (GFAP) and 4-hydroxynonenal (4-HNE) adducted proteins levels in the brains of mice with MPTP model of Parkinson's disease treated with nanozyme-laden BMM and nanozyme alone. 48 hours past MPTP administration brain tissues were harvested. Ventral midbrain areas were excised, homogenized and sonicated. Homogenates were centrifuged twice at 24,000 × g and supernatants were collected. Protein concentrations were determined using NanoDrop 2000 (Nano Drop Products, Wilmington, DE). Primary rabbit polyclonal antibodies to GFAP, ab7260 (AbCam, Cambridge, MA), were used at 1:50,000 dilution. Primary mouse monoclonal antibodies to 4-HNE adducts, MAB3249 (R&D Systems, Minneapolis, MN) were used in 1:500 dilution (in concentration 1μg/ml). The primary monoclonal chicken antibodies to β-actin (Sigma-Aldrich, St. Louis, MO), were used at 1:10,000 dilution. Secondary chicken anti-rabbit HRP-conjugated antibodies, ab 6829 (AbCam) were used in 1:4,000 dilution; secondary goat anti mouse HRP-conjugated antibodies HAF007 (R&D Systems) in were used in 1:1,000 dilution. Specific protein bands were visualized using a Immobilon Western Chemiluminescent HRP Substrate kit (Millipore, Billerica, MA). The levels of GFAP expression and 4-HNE adducts were quantitated by densitometry using Bio-Rad imaging densitometer (Bio-Rad Laboratories, Hercules, CA). To correct for loading differences, the levels of proteins were normalized to the constitutively expressed β-actin.

Immunohistochemical analyses

MPTP-intoxicated C57Bl/6 mice (18 mg/kg) were *i.v.* injected with PBS, nanozyme alone, BMM loaded with nanozyme (5×10^6 cells/mouse/100μl), or empty BMM. Healthy non-intoxicated animals injected with PBS instead of MPTP were used in a control group. Forty eight hours later animals were sacrificed and perfused according to standard perfusion protocol with PBS, followed by whole body fixation in 4% PFA in PBS. Brains were removed, washed in ice-cold PBS, post-fixed in 10% phosphate-buffered paraformaldehyde, and paraffin embedded. Immunohistochemical analysis was performed in 30 μm thick consecutive coronal brain sections. For GFAP staining, tissue sections were permeabilized with 0.01% Triton X-100 in TBS for 30 minutes and blocked for 1 hour with 10% normal goat serum (NGS, Vector Laboratories Inc., Burlingame, CA), then incubated with rabbit anti-GFAP primary polyclonal antibody (AbCam, Cambridge, MA) 1:2,500 dilution for 16 hours at 4°C. Tissue slices were incubated with goat anti-rabbit Alexa Fluor 488 secondary antibody (Invitrogen, Carlsbad, CA, 1:200 dilution) for 1 hour, and mounted on slides. Immunoreactivity was evaluated by fluorescent analysis using confocal microscope Zeiss 510 Meta Confocal Laser Scanning Microscope (Jena, Germany), and ImageJ software (NIH, Bethesda, MA). For detection of microglia activation and neurodegeneration, primary monoclonal rat anti mouse anti-CD11b antibodies (AbD Serotec, Raleigh, NC) 1:500 dilution), and secondary biotinylated goat anti-rat antibodies (Vector Laboratories, Burlingame, CA, 1:200 dilution) were used. After incubation with secondary antibodies, VecStain Elite kit (Vector Laboratories) was used according to manufacturer's directions. 3,3'-Diaminobenzidine (DAB) system was used as described [24] for immunoreactivity visualization. For the assessment of the neuroptotective effect of nanozyme formulations, mice were sacrificed seven days after the MPTP intoxication. Tyrosine hydroxylase (TH) staining was used to quantitate numbers of dopaminergic neurons. Primary rabbit anti-mouse TH antibodies (Calbiochem, San Diego, CA) were diluted 1:5000 and applied for 48 hours, secondary biotinylated goat anti-rabbit antibodies were used at a

dilution of 1:200 for one hour at room temperature, followed by application of VecStain kit and DAB.

Stereological analyses

The total number of TH-positive SN neurons and CD11b-positive microglia cells were counted by using the optical fractionator module in StereoInvestigator software (MicroBrightField, Inc., Williston, VT). In agreement with this method, TH- and CD11b-positive cells were counted within SN in the same brain hemisphere of every fourth section throughout the entire extent of the SN. Each midbrain section was viewed at low power (×10 objective), and the SN was outlined. Then, the number of stained cells was counted at high power (×100 for neurons, ×60 for microglia). Cells counts were obtained from ameboid Mac-1+ cells within the SN, and cells per mm^2 were calculated. The total numbers of TH-positive cells in the SN were calculated as previously described [25].

Levels of astrocytosis were determined in the ventral midbrain region by fluorescent analysis of GFAP expression. Quantification was performed as the function of the positive area by ImageJ software (free access provided by National Institute of Health).

Proton Magnetic Resonance Spectroscopic Imaging (^{1}H MRSI)

To assess the effect of catalase-augmented neuroprotection, neuronal N-acetylaspartate (NAA) levels in MPTP-intoxicated mice treated or untreated with nanozyme-loaded BMM were evaluated with ^{1}H MRSI as described [26]. High resolution (1 μl voxel) ^{1}H MRSI was used to delineate metabolite concentrations of NAA. Readouts were taken before and seven days after treatment, and the data was acquired on a Bruker Avance 7T/21 cm system operating at 300.41 MHz using actively decoupled 72 mm volume coil transmit and a laboratory built 1.25 × 1.5 cm receive surface coil. MR images were acquired with a 20 mm field of view (FOV), 25 contiguous 0.5 mm thick slices, interleaved slice order, 128 × 128 matrix, eight echoes, 12 ms echo spacing, refocused with CPMG phase cycled RF refocusing pulses to form eight images used for T_2 mapping which were co-registered with images of histological sections. Spectroscopic images were obtained using a numerically optimized binomial excitation [27], refocused using three orthogonal slice selective refocusing pulses (Binomial Excitation with Volume selective Refocusing, BEVR) [26]. Spectroscopic images were obtained by selecting an 8 × 4.2 × 1.5 mm volume of interest, using 24 × 24 spatial encoding over a 20 mm FOV with four averages in the slice containing the SNpc yielding a nominal voxel size of 1 μl.

Statistical analysis

For the all experiments, data are presented as the mean ± SEM. Tests for significant differences between the groups were done using one-way ANOVA with multiple comparisons (Fisher's pairwise comparisons) using GraphPad Prism 5.0 (GraphPad software, San Diego, CA). A minimum *p* value of 0.05 was estimated as the significance level for all tests.

Results

In order to develop a targeted cell-mediated delivery of catalase to the brain BMM were loaded *ex vivo* with the nanozyme, and administered intravenously (*i.v.*) (Figure 1).

BMM-nanozyme loading

Nanozyme accumulation in BMM was evaluated by catalase ^{125}I-labeling. For these experiments, cells were incubated with radioactive-labeled nanozyme and radioactive counts measured. Total radioactivity of 5×10^6 BMM collected was 238.7±19.3 CPM compared with 1 ml of labeled nanozyme containing media with 2550.0 ± 38.7 CPM of activity. This

demonstrated that BMM accumulated 9.3% of the catalase nanozyme from the media corresponding to 280 μg catalase/5×10^6 cells. These data does not preclude nanoparticles non-specifically bound to the cell surface. Therefore, the total amount of catalase injected into a mouse would be ~ 100 μl solution of nanozyme administered alone or with BMM carriers.

Nanozymes and BMM function

To deliver catalase to the site of action, the donor cells would need to maintain their biological functions. For macrophages this would include movement and secretory activities. Our previous studies indicated that nanozyme (as well as catalase or copolymer alone) was not cytotoxic [6]. *First*, nanozyme loading did not affect α4 integrin levels, a protein that allows BMM to pass into the CNS as evaluated by FACS (Figure 1S). *Second*, BMM loaded with nanozyme showed adherence and mobility across BMVEC similar to non-loaded macrophages. No effect of nanozyme loading on the basic functions tested for BMM was demonstrated (Figure 2S).

Tissue nanotoxicology

To evaluate potential nanozyme-loaded BMM toxicities, mice were injected intravenously (*i.v.*) with nanozyme-loaded BMM (Z=1), PEI-PEG alone, or with PBS as a control. Two days after the last injection, the animals were sacrificed, and the internal organs were collected at necropsy. Light microscopic examination of brain, kidney, liver, and spleen was performed on hematoxylin and eosin (H&E) stained paraffin sections. Brain tissue showed no evidence of neuronal injury, edema or breakdown of the BBB for all treatment solutions (Figure 3S). No evidence of nephrotoxicity (acute tubular necrosis, glomerular edema or fibrosis of the interstitium) could be detected in treated mice compared with controls. Liver tissue from both controls and treated animals demonstrated absence of significant hepatocyte necrosis, cholestasis, micro- or macrosteatosis, inflammatory changes in bile ducts or microvessels. No splenic morphological changes including thickening of the capsule, fibrosis, or trabeculae were noted.

TUNEL staining showed no remarkable increases in apoptosis in the brain, kidney, and liver (Figure 4S). Confocal images revealed comparable levels of TUNEL positive cells in spleen of both control and nanozyme treated animals that are within physiological levels, but not indicative of pathological processes. In fact, there was less TUNEL staining in spleen of treated animals compared to control. Overall, these results strongly suggest that injection of nanozyme-loaded BMM as well as block-copolymer alone at the doses used in these experiments did not show tissue toxicity. These studies are relevant as a number of recent publications demonstrate that macrophage migration serve as mediators for disease [28, 29].

Sustained BMM release of nanoformulated catalase

Pharmacokinetic studies of ^{125}I-labeled catalase nanozyme loaded in BMM and *i.v.* injected into healthy C57Bl/6 mice discriminated amounts of nanozyme in peripheral blood plasma and the cell fraction (Figure 2). Drastic differences between catalase nanozyme administered in the cell carriers or alone were found. Thus, relatively high levels of radiolabeled catalase in the plasma were recorded over 168 hours after administration of nanozyme to BMM (Figure 2A). In contrast, radiolabeled catalase in the plasma of animals injected with nanozyme alone was significantly lower and sharply declined over the study period. Furthermore, the cell pellet fraction from blood samples taken from animals injected BMM-loaded with radiolabeled nanozyme showed decrease radioactivity suggesting that BMM gradually release catalase nanozyme (Figure 2B). The cell pellet obtained from blood of mice injected with nanozyme alone has very little (if any) amount of ^{125}I-labeled catalase. To evaluate numbers of cell carriers in blood, radioactive labeled BMM loaded with non-labeled nanozyme were injected *i.v.* into healthy mice (Figure 2C). It was clearly demonstrated that the total number of the

loaded BMM in the blood decreased over time. This suggests that at least a portion of BMM loaded with nanozyme migrate from the blood away into the tissue and the tissue-associated BMM slowly unload and supply the blood plasma providing sustained levels of catalase in the plasma over seven days.

To support these data, we studied release of catalase nanozyme from BMM *in vitro.* The loaded BMM released catalase in the external media for at least 20 days (Figure 5S), suggesting that loaded and transferred cells might be a depot for the sustained release of nanoformulated catalase *in vivo.*

Biodistribution of BMM-carried nanozymes in MPTP-intoxicated mice

To examine whether nanozyme-loaded BMM reach the brain and deliver their payload, image visualization and infrared spectroscopy studies (IVIS) were conducted in MPTP mice. Non-labeled BMM loaded with fluorescent-labeled nanozyme were administered *i.v.* to MPTP-intoxicated mice. In parallel experiments, the non-labeled nanozyme was loaded into fluorescently-labeled cell carriers and injected into MPTP-treated mice. Fluorescent and light images of dorsal and ventral planes of the injected animals were taken at various times. Both components of the formulation, nanozyme and BMM, were detected in the brain area of the animals (Figures 3A and B). In addition, both planar images revealed accumulation of nanozyme as well as cell carriers in the peritoneal area, most likely corresponding to the liver and spleen uptake (Figures 3A, B and 5S-A, B). As expected, both nanozyme (Figure 3A) and BMM (Figure 3B) appeared in the brain within the first two hours after the injection, suggesting cell-mediated transport of catalase, although, fluorescent activity in mice receiving labeled cells with non-labeled nanozyme remained at later time points compared with mice receiving labeled nanozyme loaded into non-labeled cells. Thus, labeled BMM can be found even at 48-hours (Figure 3B); whereas fluorescence in mice receiving labeled nanozyme in BMM was not detectable by 24 hours after injection (Figure 3A). Furthermore, the dorsal images reveal that transferred BMM were detected in liver at greater levels (compared to the brain, Figure 3B) than labeled nanozyme administered with BMM (Figure 3A). This might indicate that at least some portion of nanozyme was released from the cell carriers into the peripheral circulation and then reach the brain independently from the cell- carriers.

Furthermore, nanozyme administered alone (without cell carriers) was cleared from the brain much faster, typically by two hours (Figure 3C), compared with nanozyme loaded into BMM (Figure 3A). However, we cannot exclude that recording of detectable levels of catalase loaded into BMM in the brain at later time points might be due to a higher local concentration of the dye on the protein loaded into the cell-carriers, compared to the nanozyme injected alone. Noteworthy, the imaging in the living animals does not allow distinguishing between nanozyme in the blood stream or in the brain parenchyma.

To eliminate this factor, MPTP-intoxicated mice were injected with the same formulations (non-labeled nanozyme loaded into fluorescently-labeled BMM (Figure 4A); and non-labeled BMM loaded with fluorescently-labeled nanozyme (Figure 4B). Rhodamine was used as a fluorescent dye in these studies. Following injections, mice were sacrificed and perfused as described above. Confocal images of slides of selected organs (spleen, liver and brain (substantia nigra area)) taken from MPTP-intoxicated mice after adoptive transfer of fluorescently-labeled BMM confirmed results obtained by IVIS (Figures 4, 6S). Representative images from N=4 animals demonstrate detectable amounts of BMM (Figure 4A) and catalase (Figure 4B) in the brain, although, at substantially lower levels than in the liver and spleen. Noteworthy, healthy (non-MPTP-intoxicated) mice had no fluorescently-labeled macrophages in the brain and much less amount in the liver (Figure 7S). All together this data provide initial evidence that adoptive transfer of nanozyme loaded BMM can increase the delivery of the

enzyme to the brain as well as other peripheral tissues known to be sites of macrophage tissue migration.

Nanozyme-loaded BMM reduce SN neuroinflammation

Linkages between neuroinflammation and nigrostriatal degeneration in PD were previously reported [30]. Therefore, decreasing inflammation may provide a protective effect on dopaminergic neurons after MPTP intoxication [31,32]. In order to assess the levels of inflammation in the brain, we evaluated microglial activation and astrocytosis in the MPTP model. Expression of two neuroinflammation markers, CD11b (for reactive microglia), and GFAP (for astrosytes) was assessed. Five groups of animals were evaluated: i) naive, non-intoxicated mice injected with PBS ii) MPTP-intoxicated mice; and iii) MPTP-intoxicated mice treated with nanozyme-loaded BMM; iv) MPTP-intoxicated mice treated with nanozyme alone; and v) MPTP-intoxicated mice treated with non-loaded BMM. Two days after injection of MPTP or PBS, brains were removed and CD11b and GFAP levels assessed by immunohistochemistry.

MPTP intoxication upregulated expression of CD11b by reactive microglia within the SN as exhibited a more amoeboid morphology in MPTP-treated mice compared to ramified microglia in PBS-treated mice (Figure 5A). Treatment of MTP-intoxicated mice with nanozyme-loaded BMM resulted in decreased levels of CD11b and 50 % less activated microglia cells compared with MPTP-intoxicated control animals (Figure 5). Representative images demonstrated more resting microglia with cell bodies barely visible and only few fine ramified processes (sent out branches). This signifies that catalase nanoparticles loaded into monocytes can prevent MPTP-induced nigrostriatal neuroinflammation. Interesting, nanozyme administered alone produced similar decreases in microglial activation and astrocytosis in the SNpc, as nanozyme loaded into macrophages. No effect on SN neuroinflammation was observed in mice injected with MPTP and unlabeled BMM compared with those injected with MPTP alone.

Similarly to microglial activation, MPTP injections caused increase in GFAP expression levels assessed by western blot analysis (Figure 6). In contrast, treatment of MPTP-injected mice with catalase-loaded monocytes resulted in decreased GFAP levels. Noteworthy, reduction of astrocytosis also was recorded when nanozyme was injected without cell-carriers. No effect was detected following injection of empty BMM. Similar trend was observed with GFAP expression levels assessed by immunohistochemistry on brain slides, although the differences were not statistically significant. MPTP treatment increased GFAP expression in SN compared with that of PBS-treated mice, whereas transfer of nanozyme-loaded BMM as well as nanozyme administered alone diminished MPTP-induced astrocytosis. MPTP-intoxicated mice treated with empty BMM (data not shown).

Nanozyme-loaded BMM decrease oxidative stress in midbrain in MPTP mice

4-Hydroxynonenal (4-HNE) is known to be generated due to the increase in the lipid peroxidation chain reaction in PD [33,34]. To evaluate effects of nanozyme formulations on oxidative stress, we assessed expression levels of 4-HNE in five animal groups: i) naive, non-intoxicated mice injected with PBS; ii) MPTP-intoxicated mice; and iii) MPTP-intoxicated mice treated with nanozyme-loaded BMM; iv) MPTP-intoxicated mice treated with nanozyme alone; and v) MPTP-intoxicated mice treated with non-loaded BMM. The expression levels of all bands were evaluated by western blot (Figure 8S). The obtained data confirmed results for the effects on neuroinflammation described above. It was clearly demonstrated that MPTP injections caused more than 3-fold increase in 4-HNE levels compared to healthy animals. Treatment of MPTP-intoxicated mice with catalase nanozyme loaded into the cells, as well as nanozyme alone decreased oxidative stress. No effect on lipid peroxidation was detected after treatment with empty BMM.

Nanozymes and neuroprotective responses in MPTP mice

The neuropathology associated with PD involves brain inflammation, microglial activation, subsequent secretion of neurotoxic factors, followed by increased ROS production that play crucial roles in dopaminergic cell damage and death [31,32,35,36]. The demonstration of attenuated MPTP-induced inflammatory responses by catalase administered in BMM suggested a putative protective role against neurodegeneration for nigrostriatal dopaminergic neurons. Therefore, histological analyses (striatal densitometric and nigral stereological analyses) were performed for five groups of mice similar to neuroinflammation studies: i) non-intoxicated mice injected with PBS; ii) MPTP-intoxicated mice; iii) MPTP-intoxicated mice treated with nanozyme-loaded BMM; iv) MPTP-intoxicated mice treated with nanozyme alone; and v) MPTP-intoxicated mice treated with empty BMM. MPTP intoxication decreased the number of TH-positive nigral dopaminergic neurons (32 % survival) compared to PBS-treated controls (Figure 7, **second bar**). In contrast, the number of surviving dopaminergic neurons in MPTP-intoxicated mice treated with nanozyme-loaded BMM was greater than the total number of neurons in MPTP-treated mice (62.4 % survival) (Figure 7B, **third bar**). Furthermore, treatment with nanozyme alone (without cell carriers, Figure 7B, **fourth bar**) also produced some neuroprotection effect, although with fewer neurons (41.3 % survival) compared to the mice treated with cell/nanozyme formulation. Finally, treatment with empty monocytes did not preserve neurons in MPTP-intoxicated animals (31.1 % survival) (Figure 7B, **fifth bar**). This signified a neuroprotective effect of catalase-loaded monocytes in MPTP-induced neurodegeneration.

^{1}H MRSI and neuroprotective responses for nanozyme-loaded BMM

To evaluate the neuroprotective effect, MPTP-intoxicated mice were injected *i.v.* with nanozyme-loaded BMM, and seven days later levels of N-acetylaspartate (NAA) within the SN and striatum were assessed by ^{1}H MRSI. To control for inter-animal variability of NAA concentrations, each mouse was scanned before MPTP treatment and NAA levels normalized as the difference between pre-treatment levels and those seven days post-treatment (Figure 8). MPTP-intoxication caused significant loss of NAA in SN and striatum. In contrast, no reduction in NAA levels were detected in MPTP-intoxicated mice treated with nanozyme-loaded BMM. This indicates that catalase nanozyme-loaded BMM have a neuroprotective capacity during MPTP-induced dopaminergic neurodegeneration preventing inflammation in the SN and stratum of MPTP-treated mice and as a result increasing neuronal survival upon MPTP intoxication.

Discussion

Neuroinflammation is a common pathogenic event underlying a broad range of neurological diseases. This includes PD, Alzheimer's disease, prion disease and HIV-1 associated dementia. In particular, PD is characterized by microglial activation, release of cytokines, such as TNF-α, interleukin-1 (IL-1), and interferon-γ (IFN-γ), and chemokines that lead to the profound damage of surrounding tissue by reactive oxygen species (ROS), in particular, dopaminergic neuronal loss in SNpc [37–40]. The death of dopaminergic neurons causes further microglia activation and subsequent escalation of neurodegeneration. Antioxidants are capable of decreasing the level of tissue damage by ROS scavenging, and therefore produce therapeutic effects in inflamed tissues. For example, catalase, the enzyme that converts hydrogen peroxide into water and oxygen with one of the highest turnover rates, was used in numerous works as an active agent of antioxidative formulations [41,42]. Many studies have shown that reduction of the oxidative stress-related damage, including ROS-scavenging, are attractive strategies for *in vivo* and *in vitro* models of PD with the possible future translation to clinics [2,43]. However, many promising approaches fail to show benefits in humans, because the BBB severely limits delivery of therapeutic polypeptides to the brain and is a major obstacle to the successful

treatment of many devastating central nervous system (CNS) diseases [44,45]. Therefore, brain inflammation commonly detected in patients with PD can be used as a target for cell-mediated delivery of catalase to sites of CNS inflammation and injury. Utilizing the common approach to oxidative stress, we developed a novel cell-based drug delivery system of antioxidants that features tissue specificity, efficient penetration of the BBB, and potential for clinical translation (Figure 1, **Pathway I**).

Using BMM as a carrier system for delivery of therapeutic proteins to the brain offers advantages that include: i) a prolonged drug circulation in the blood stream, ii) a time-controlled release of a loaded drug, iii) a possibility of targeted drug transport to the site of action, and finally, iv) decreased drug immunogenicity. Noteworthy, BMM have been utilized as a delivery system for antiretroviral therapy of HIV in mice [16,46]. Indinavir, a protease inhibitor used to treat HIV infection, was packaged into nanosuspension and then loaded into BMM. The loaded cell carriers were transferred into HIV-1-infected, humanized immune-deficient mice. A single dose of indinavir using BMM as a carrier was demonstrated to reduce numbers of virus-infected cells in plasma, lymph nodes, spleen, liver, and lungs, as well as protect CD4+ T cells. Sustained antiretroviral therapeutic responses with concomitant immune reconstitution were seen for up to 14 days.

However, this new concept raises numerous questions and concerns. Some of these concerns include the ability of monocyte-macrophages to accumulate substantial amount of catalase nanoparticles and release them at the site of action; preservation of catalase enzymatic activity inside the cell carriers; and the ability of catalase released from cell carriers to inactivate microglial-produced ROS were previously addressed [6]. This study further makes an effort to address some of these issues. *First*, it is known that in order to infiltrate the brain, monocytes utilize specific mechanisms; adhesion to endothelial cells of brain capillaries. Therefore, we examined the ability of BMM loaded with the drug to sustain their basic properties, *i.e.* adherence and migratory activity, required for the drug delivery mission. The data indicated that loading of catalase nanozyme did not affect the ability of monocytes to adhere to and cross BBB endothelial cell monolayers.

Another obvious concern for monocyte-macrophage based drug delivery relates to possible cytotoxic effects of cell-carriers for target organs. Monocyte-macrophages attracted to the site of pathology by cytokines are known to release ROS that cause cell damage. Moreover, a number of therapeutic strategies for CNS neurodegenerative disorders are based on the prevention of monocyte-macrophage infiltration [47]. To address this concern, we performed histopathological and apoptosis assessments for the main organs in healthy mice injected with nanozyme-loaded BMM. The results revealed no toxicity in the spleen, liver, kidney, and brain *in vivo* at doses used in these studies.

Cell carriers provided high sustained levels of plasma catalase nanozyme over seven days suggesting a depot role for the therapeutic enzyme. Biodistribution studies of radioactively-labeled catalase nanozyme injected in BMM or alone distinguished between catalase in plasma and cellular catalase. Indeed, cell fractions separated from blood of animals injected with nanozyme loaded into BMM showed high radioactivity levels decreasing over study time period. In contrast, little (if any) catalase were detected in cell fractions from peripheral blood of animals injected with catalase nanozyme alone. This suggests that adoptively transferred BMM gradually released catalase into the blood stream. Thus, loaded with nanozyme macrophages released catalase over 20 days in *in vitro* experiments. These might be the cells circulating in the blood stream, as well as the cells that migrated from the blood into the tissue and supplying the blood plasma with sustained levels of catalase. This is especially important for chronic conditions of PD.

Next, we determined the extent of nigrostriatial ingress of fluorescently labeled BMM loaded with nanozyme, as well as fluorescently-labeled nanozyme loaded in the cells in a murine model of nigrostriatal degeneration by IVIS studies. Nanozyme-loaded BMM were transferred *i.v.* to mice with active neuroinflammatory responses induced by MPTP, and were tracked using IVIS. Cell carriers as well as the enzyme were detected in the brain within the first hours after transfer, suggesting that BMM loaded with catalase might reach CNS and deliver catalase to the inflammatory site (Figure 1, **Pathway I**). Furthermore, significant numbers of the cells were detected in spleen and liver that might be attributed to inflammation caused by MPTP injections or due to host vs. graft responses [22]. Interestingly, the biodistribution kinetics for nanozyme and cell carriers were slightly different. Thus, BMM appeared in the brain to a lesser extend compared to the liver and spleen, than nanozyme. Moreover, BMM were recorded in the brain for longer time points (up to 24 hours) compared with nanozyme (up to 7 hours). This might indicate that at least a fraction of the nanozyme was released from the monocytes to the blood stream and distributed independently (Figure 1, **Pathway II**). To this end, we do not exclude the possibility of using another pro-inflammatory responsive cell such as T cells or dendritic cells for nanozyme delivery. In fact, mixed populations of drug carriers might have advantages including cell activation and different biodistribution kinetics. We also cannot exclude that the nanozyme released by BMM may be taken up by circulating monocytes as well as monocytes in the liver, for example, and then carried to the brain. The detailed mechanism of drug transport to the brain is to be examined.

The most consistent pathological finding in PD is selective loss of dopaminergic neurons within the SNpc with little effect on surrounding neurons. Although the etiology of PD remains enigmatic, mounting evidence indicates neuroinflammation as a major contributing factor in progressive dopaminergic neurodegeneration. Therefore, the major question, whether catalase nanozyme administered in BMM carriers was able to produce a neuroprotective effect in MPTP-intoxicated mice was divided into two parts: i) decrease of neuroinflammation, and ii) increase of dopaminergic neuron survival. The level of inflammation was evaluated using markers for activated microglia and astroglia. The neurotoxin MPTP causes a severe and irreversible parkinsonian syndrome in humans and in nonhuman primates [48], whereby an initial time-limited insult initiates a self-perpetuating process of nigrostriatal neurodegeneration [49]. In mice, MPTP reproduces most of the biochemical and pathological hallmarks of PD, including specific degeneration of dopaminergic neurons that originate in the SNpc and enervate the striatum [50]. It was clearly demonstrated that treatment of MPTP-intoxicated mice with nanozyme-loaded cells resulted in amelioration of microglial activation and astrocytosis in SNpc. In particular, two-fold reduction in CD11b levels for activated microglia compared with MPTP-intoxicated animals were observed. Similar effect of nanozyme formulations was demonstrated for oxidative stress in midbrain. This suggests that injections of catalase nanozyme in BMM carriers were sufficient to inactivate ROS after MPTP intoxication.

Finally, the neuroprotective effect of catalase-loaded BMM in MPTP-induced neurodegeneration was quantified by histological analysis along with ^{1}H MRSI analysis. Both techniques indicated significant neuronal loss in SNpc of MPTP intoxicated mice. In contrast, no reduction in dopaminergic neurons was observed in MPTP-intoxicated mice treated with nanozyme-loaded BMM on day seven after therapy by MRSI. Histological analysis indicated that TH+ nigral neurons were significantly reduced in MPTP-treated mice, whereas in mice treated with monocytes loaded with catalase nanozyme, the numbers of TH+ nigral neurons were visibly and significantly higher. Noteworthy, treatment of MPTP-intoxicated mice with nanozyme alone (as well as empty cell-carriers) did not significantly increase the amount of TH+ neurons. This indicates that nanozyme-loaded BMM have a profound neuroprotective capacity in a murine PD model. Interestingly, treatment of MPTP-intoxicated mice with nanozyme alone (without cell carriers) or nanozyme loaded into monocytes decreased

microglial activation in SNpc at the same extent. At the same time, neuroprotective effect of nanozyme loaded in cell-carriers was significantly greater than those of nanozyme administered alone. We suggest that staining for Mac-1 reflects only fraction of ROS production, and therefore might not account for all damage caused by MPTP intoxications to dopaminergic neurons.

In terms of using this type of therapy in a clinical setting, we consider using monocytes derived from peripheral blood or bone marrow of the patients as cell carriers. For example, monocytes can be harvested from peripheral blood by apheresis, loaded with catalase nanoparticles, and re-infused into the patient. An alternative approach may be harvesting monocytes from bone marrow, which will allow for expansion of monocyte population, although this would require a more invasive procedure and extra time. Furthermore, catalase loading into monocytes might be significantly increased by conjugation of the polymer with monocyte receptor-specific moieties (e.g., folate, gelatin, fibronectin, A-protein, mannose, or RGD peptide) that will promote their targeting to monocyte scavenger receptors, or with antibodies to CD11b. Ideally, injected *i.v.* targeted catalase nanoparticles would be selectively taken up by circulating cell carriers directly from the peripheral blood.

The last scenario seems to be the most realistic; especially taking into account the fact that catalase nanozyme administered alone produced the same level anti-inflammatory effect in MPTP-intoxicated mice as nanozyme-loaded into the cell-carriers. This may indicate that nanozyme-loaded BMM release at least a portion of catalase in the blood stream and then nanozyme reaches CNS independently of cell-carriers (Figure 1, **Pathway II**). Another possibility is that *i.v.* injected nanozyme (without cells) is taken by circulating host monocytes, which deliver catalase to SNpc by the same route as transferred BMM shown in these studies (Figure 1, **Pathway I**). Finally, it has been demonstrated that along with microglia, peripheral immune-response cells (monocytes, macrophages, T cells, etc.) can also play an essential role in brain inflammation in PD [51,52]. To this end, catalase released from cell-carriers in the liver or spleen (the most enriched organs after transfer of nanozyme-loaded BMM) might produce suppression of peripheral leukocyte activation and result in significant protection of nigrostratial neurons against MPTP-induced neurodegeneration [52,53] (Figure 1, **Pathway III**). The most likely explanation, however, reflects the acute nature of the MPTP model and the fact that a single level of catalase may in fact be sufficient to attenuate neuroinflammation and lead to neuroprotection in this model. More detailed mechanistic studies are ongoing in our laboratory including the use of chronic MPTP model systems that are perhaps most reflective of human disease chronicity.

CONCLUSIONS

Overall, these studies demonstrated the feasibility of a therapeutic approach using cell-mediated catalase delivery for neuroprotection of dopaminergic neurons in a mouse model of PD. Therefore, we suggest the utilization of these cells as carriers of therapeutic formulations due to their ability to efficiently engulf particles, penetrate the BBB, and reach the site of neuropathology.

SUMMARY POINTS

- Nanoformulated catalase (nanozyme) obtained by coupling the enzyme to a synthetic polyelectrolyte of opposite charge was loaded into bone marrow derived monocytes (BMM) for cell-mediated transport to CNS.
- BMM delivery of nanozyme showed sustained and prolonged release of the enzyme in plasma.

- Biodistribution studies suggest that nanozyme-loaded BMM might release a portion of catalase in the blood stream, which then nanozyme reaches CNS independently of cell-carriers.
- Therapeutic efficacy of the nanozyme loaded BMM was confirmed by reductions in microglial activation and astrocytosis in MPTP-intoxicated mice.
- Neuroprotection by the nanozyme loaded BMM in MPTP-induced neurodegeneration was demonstrated by increased survival of dopaminergic neurons and increased nigrostriatal NAA levels by magnetic resonance spectroscopic imaging.
- The studies demonstrated the feasibility of the approach using cell-mediated catalase delivery for neuroprotection of dopaminergic neurons in a mouse model of PD.

Supplementary Material

Refer to Web version on PubMed Central for supplementary material.

Acknowledgments

This study was supported by the National Institutes of Health grants 1RO1 NS057748 (EVB), 2R01 NS034239 (HEG), 2R37 NS36126 (HEG), P01 NS31492 (HEG), P20RR 15635 (HEG), P01 MH64570 (HEG), P01 NS43985 (HEG), and RR021937 (AVK). We are grateful to Anita Jennings (Molecular Phenotyping Core Facility, UNMC) for her invaluable help and opinion with histochemical analysis; Janice A. Taylor and James R. Talaska (Confocal Laser Scanning Microscope Core Facility, UNMC) for providing assistance with confocal microscopy and the Nebraska Research Initiative and the Eppley Cancer Center for their support of the Core Facility; and Ashley Reynolds for her expert advices in data analysis.

REFERENCES

1. Lees, Aj; Hardy, J.; Revesz, T. Parkinson's disease. Lancet 2009;373(9680):2055–2066. [PubMed: 19524782]
2. Gonzalez-Polo, Ra; Soler, G.; Rodriguezmartin, A.; Moran, Jm; Fuentes, Jm. Protection against mpp + neurotoxicity in cerebellar granule cells by antioxidants. Cell Biol Int 2004;28(5):373–380. [PubMed: 15193280]
3. Jain S, Mishra V, Singh P, Dubey Pk, Saraf Dk, Vyas Sp. Rgd-anchored magnetic liposomes for monocytes/neutrophils-mediated brain targeting. Int J Pharm 2003;261(1–2):43–55. [PubMed: 12878394]
4. Kao, Wj; Liu, Y.; Gundloori, R., et al. Engineering endogenous inflammatory cells as delivery vehicles. J Control Release 2002;78(1–3):219–233. [PubMed: 11772463]
5. Begley, Dj. Delivery of therapeutic agents to the central nervous system: The problems and the possibilities. Pharmacol Ther 2004;104(1):29–45. [PubMed: 15500907]
6. Batrakova, Ev; Li, S.; Reynolds, Ad, et al. A macrophage-nanozyme delivery system for parkinson's disease. Bioconjug Chem 2007;18(5):1498–1506. [PubMed: 17760417] ** of considerable interest: This manuscript reported development and characterization of cell-mediated delivery system of antioxidant enzyme, catalase. Loading, release, and protection of enzymatic activity of catalase in bone marrow-derived monocytes (BMM) are evaluated in *in vitro* model of PD.
7. Lossinsky, As; Shivers, Rr. Structural pathways for macromolecular and cellular transport across the blood-brain barrier during inflammatory conditions. Review. Histol Histopathol 2004;19(2):535–564. [PubMed: 15024715]
8. Pawlowski, Na; Kaplan, G.; Abraham, E.; Cohn, Za. The selective binding and transmigration of monocytes through the junctional complexes of human endothelium. J Exp Med 1988;168(5):1865–1882. [PubMed: 3183575]
9. Kuby, J. Immunology. New York: Freeman, WH. and Co; 1994.

10. Daleke, Dl; Hong, K.; Papahadjopoulos, D. Endocytosis of liposomes by macrophages: Binding, acidification and leakage of liposomes monitored by a new fluorescence assay. Biochim Biophys Acta 1990;1024(2):352–366. [PubMed: 2162207]
11. Lee, Kd; Hong, K.; Papahadjopoulos, D. Recognition of liposomes by cells: In vitro binding and endocytosis mediated by specific lipid headgroups and surface charge density. Biochim Biophys Acta 1992;1103(2):185–197. [PubMed: 1543703]
12. Nishikawa K, Arai H, Inoue K. Scavenger receptor-mediated uptake and metabolism of lipid vesicles containing acidic phospholipids by mouse peritoneal macrophages. J Biol Chem 1990;265(9):5226–5231. [PubMed: 2318890]
13. Fujiwara M, Baldeschwieler Jd, Grubbs Rh. Receptor-mediated endocytosis of poly(acrylic acid)-conjugated liposomes by macrophages. Biochim Biophys Acta 1996;1278(1):59–67. [PubMed: 8611608]
14. Nguyen, Hk; Lemieux, P.; Vinogradov, Sv, et al. Evaluation of polyether-polyethyleneimine graft copolymers as gene transfer agents. Gene Ther 2000;7(2):126–138. [PubMed: 10673718]
15. Vinogradov S, Bronich T, Kabanov A. Self-assembly of polyamine-poly(ethylene glycol) copolymers with phosphorothioate oligonucleotides. Bioconjugate Chemistry 1998;9(6):805–812. [PubMed: 9815175]
16. Dou H, Destache Cj, Morehead Jr, et al. Development of a macrophage-based nanoparticle platform for antiretroviral drug delivery. Blood 2006;108(8):2827–2835. [PubMed: 16809617]
17. Seguin R, Biernacki K, Rotondo Rl, Prat A, Antel Jp. Regulation and functional effects of monocyte migration across human brain-derived endothelial cells. J Neuropathol Exp Neurol 2003;62(4):412–419. [PubMed: 12722833]
18. Zelivyanskaya, Ml; Nelson, Ja; Poluektova, L., et al. Tracking superparamagnetic iron oxide labeled monocytes in brain by high-field magnetic resonance imaging. J Neurosci Res 2003;73(3):284–295. [PubMed: 12868062]
19. Weidenfeller C, Schrot S, Zozulya A, Galla Hj. Murine brain capillary endothelial cells exhibit improved barrier properties under the influence of hydrocortisone. Brain Res 2005;1053(1–2):162–174. [PubMed: 16040011]
20. Batrakova E, Han H, Miller D, Kabanov A. Effects of pluronic p85 unimers and micelles on drug permeability in polarized bbmec and caco-2 cells. Pharm Res 1998;15(10):1525–1532. [PubMed: 9794493]
21. Batrakova E, Li S, Miller D, Kabanov A. Pluronic p85 increases permeability of a broad spectrum of drugs in polarized bbmec and caco-2 cell monolayers. Pharm Res 1999;16(9):1366–1372. [PubMed: 10496651]
22. Benner, Ej; Mosley, Rl; Destache, Cj, et al. Therapeutic immunization protects dopaminergic neurons in a mouse model of parkinson's disease. Proc Natl Acad Sci U S A 2004;101(25):9435–9440. [PubMed: 15197276]
23. Jackson-Lewis V, Przedborski S. Protocol for the mptp mouse model of parkinson's disease. Nat Protoc 2007;2(1):141–151. [PubMed: 17401348]
24. Tieu K, Perier C, Caspersen C, et al. D-beta-hydroxybutyrate rescues mitochondrial respiration and mitigates features of parkinson disease. J Clin Invest 2003;112(6):892–901. [PubMed: 12975474]
25. Liberatore, Gt; Jackson-Lewis, V.; Vukosavic, S., et al. Inducible nitric oxide synthase stimulates dopaminergic neurodegeneration in the mptp model of parkinson disease. Nat Med 1999;5(12):1403–1409. [PubMed: 10581083]
26. Boska, Md; Lewis, Tb; Destache, Cj, et al. Quantitative 1h magnetic resonance spectroscopic imaging determines therapeutic immunization efficacy in an animal model of parkinson's disease. J Neurosci 2005;25(7):1691–1700. [PubMed: 15716405]
27. Hetherington, Hp; Pan, Jw; Mason, Gf, et al. 2d 1h spectroscopic imaging of the human brain at 4.1 t. Magn Reson Med 1994;32(4):530–534. [PubMed: 7997121]
28. Glass, Jd; Fedor, H.; Wesselingh, Sl; Mcarthur, Jc. Immunocytochemical quantitation of human immunodeficiency virus in the brain: Correlations with dementia. Ann Neurol 1995;38(5):755–762. [PubMed: 7486867]

29. Liu B, Hong Js. Role of microglia in inflammation-mediated neurodegenerative diseases: Mechanisms and strategies for therapeutic intervention. J Pharmacol Exp Ther 2003;304(1):1–7. [PubMed: 12490568]
30. Stone, Dk; Reynolds, Ad; Mosley, Rl; Gendelman, He. Innate and adaptive immunity for the pathobiology of parkinson's disease. Antioxid Redox Signal. 2009
31. Ebadi M, Srinivasan Sk, Baxi Md. Oxidative stress and antioxidant therapy in parkinson's disease. Prog Neurobiol 1996;48(1):1–19. [PubMed: 8830346]
32. Wu, Dc; Teismann, P.; Tieu, K., et al. Nadph oxidase mediates oxidative stress in the 1-methyl-4-phenyl-1,2,3,6-tetrahydropyridine model of parkinson's disease. Proc Natl Acad Sci U S A 2003;100 (10):6145–6150. [PubMed: 12721370]
33. Navarro A, Boveris A. Brain mitochondrial dysfunction and oxidative damage in parkinson's disease. J Bioenerg Biomembr 2009;41(6):517–521. [PubMed: 19915964]
34. Zarkovic N. 4-hydroxynonenal as a bioactive marker of pathophysiological processes. Mol Aspects Med 2003;24(4–5):281–291. [PubMed: 12893006]
35. Mcgeer, Pl; Itagaki, S.; Boyes, Be; Mcgeer, Eg. Reactive microglia are positive for hla-dr in the substantia nigra of parkinson's and alzheimer's disease brains. Neurology 1988;38(8):1285–1291. [PubMed: 3399080]
36. Busciglio J, Yankner Ba. Apoptosis and increased generation of reactive oxygen species in down's syndrome neurons in vitro. Nature 1995;378(6559):776–779. [PubMed: 8524410]
37. Boje, Km; Arora, Pk. Microglial-produced nitric oxide and reactive nitrogen oxides mediate neuronal cell death. Brain Res 1992;587(2):250–256. [PubMed: 1381982]
38. Chao, Cc; Hu, S.; Molitor, Tw; Shaskan, Eg; Peterson, Pk. Activated microglia mediate neuronal cell injury via a nitric oxide mechanism. J Immunol 1992;149(8):2736–2741. [PubMed: 1383325]
39. Mcguire, So; Ling, Zd; Lipton, Jw; Sortwell, Ce; Collier, Tj; Carvey, Pm. Tumor necrosis factor alpha is toxic to embryonic mesencephalic dopamine neurons. Exp Neurol 2001;169(2):219–230. [PubMed: 11358437]
40. Whitton, Ps. Inflammation as a causative factor in the aetiology of parkinson's disease. Br J Pharmacol 2007;150(8):963–976. [PubMed: 17339843]
41. Simone, Ea; Dziubla, Td; Colon-Gonzalez, F.; Discher, De; Muzykantov, Vr. Effect of polymer amphiphilicity on loading of a therapeutic enzyme into protective filamentous and spherical polymer nanocarriers. Biomacromolecules 2007;8(12):3914–3921. [PubMed: 18038999]
42. Siwale, Rc; Oettinger, Cw; Balakrishna Pai, S., et al. Formulation and characterization of catalase in albumin microspheres. J Microencapsul 2008:1–9.
43. Prasad, Kn; Cole, Wc; Hovland, Ar, et al. Multiple antioxidants in the prevention and treatment of neurodegenerative disease: Analysis of biologic rationale. Curr Opin Neurol 1999;12(6):761–770. [PubMed: 10676761]
44. Beal, Mf; Matthews, Rt. Coenzyme q10 in the central nervous system and its potential usefulness in the treatment of neurodegenerative diseases. Mol Aspects Med 1997;18:S169–S179. [PubMed: 9266519]
45. Zhao K, Luo G, Giannelli S, Szeto Hh. Mitochondria-targeted peptide prevents mitochondrial depolarization and apoptosis induced by tert-butyl hydroperoxide in neuronal cell lines. Biochem Pharmacol 2005;70(12):1796–1806. [PubMed: 16216225]
46. Dou H, Grotepas Cb, Mcmillan Jm, et al. Macrophage delivery of nanoformulated antiretroviral drug to the brain in a murine model of neuroaids. J Immunol 2009;183(1):661–669. [PubMed: 19535632] * of interest: in this study BMM have been utilized as a delivery system for antiretroviral therapy of HIV in mice.
47. Hendriks, Jj; Teunissen, Ce; De Vries, He; Dijkstra, Cd. Macrophages and neurodegeneration. Brain Res Brain Res Rev 2005;48(2):185–195. [PubMed: 15850657]
48. Langston, Jw; Irwin, I. Mptp: Current concepts and controversies. Clin Neuropharmacol 1986;9(6): 485–507. [PubMed: 3542203]
49. Langston, Jw; Forno, Ls; Tetrud, J.; Reeves, Ag; Kaplan, Ja; Karluk, D. Evidence of active nerve cell degeneration in the substantia nigra of humans years after 1-methyl-4-phenyl-1,2,3,6-tetrahydropyridine exposure. Ann Neurol 1999;46(4):598–605. [PubMed: 10514096]

50. Schmidt N, Ferger B. Neurochemical findings in the mptp model of parkinson's disease. J Neural Transm 2001;108(11):1263–1282. [PubMed: 11768626]

51. Kokovay E, Cunningham La. Bone marrow-derived microglia contribute to the neuroinflammatory response and express inos in the mptp mouse model of parkinson's disease. Neurobiol Dis 2005;19 (3):471–478. [PubMed: 16023589]

52. Mosley R, Benner E, Kadiu I, et al. Neuroinflammation, oxidative stress, and the pathogenesis of parkinson's disease. Clinical Neuroscience Research 2006;6(5):261–281. [PubMed: 18060039]

53. Audoy-Remus J, Richard Jf, Soulet D, Zhou H, Kubes P, Vallieres L. Rod-shaped monocytes patrol the brain vasculature and give rise to perivascular macrophages under the influence of proinflammatory cytokines and angiopoietin-2. J Neurosci 2008;28(41):10187–10199. [PubMed: 18842879]

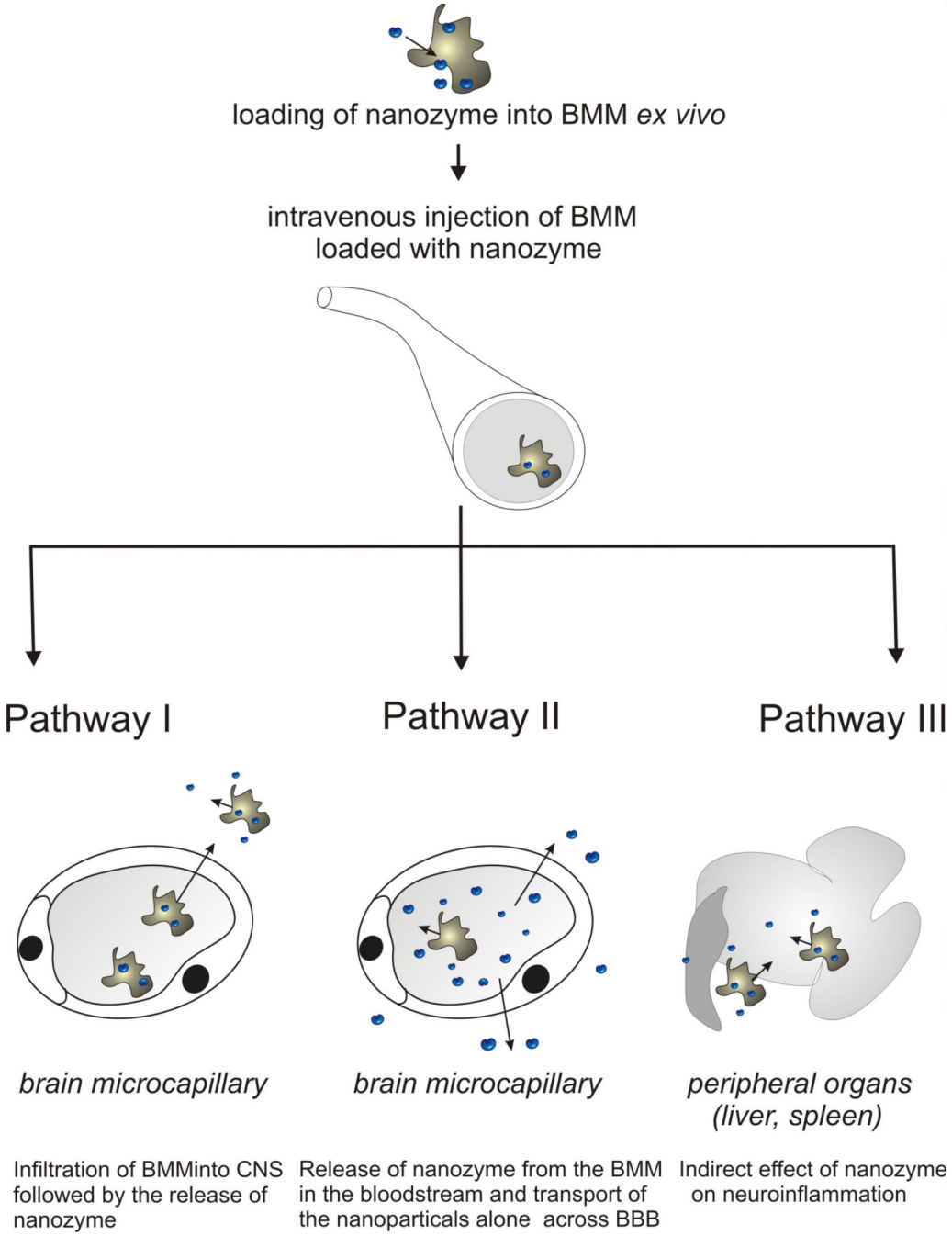

Figure 1. A pictorial scheme for cell-based nanoformulated drug delivery

Three possible ways of BMM-mediated therapeutic effects of catalase nanozyme in PD mouse model: **Pathway I**: BMM loaded with nanozyme cross the BBB and release catalase in the SNpc; **Pathway II:** nanozyme is released from BMM to the blood stream and bypasses the BBB independently of cell-carriers; **Pathway III:** BMM-released catalase nanozyme in the liver and spleen suppresses peripheral leukocyte activation that results in significant protection of nigrostratial neurons against MPTP-induced neurodegeneration.

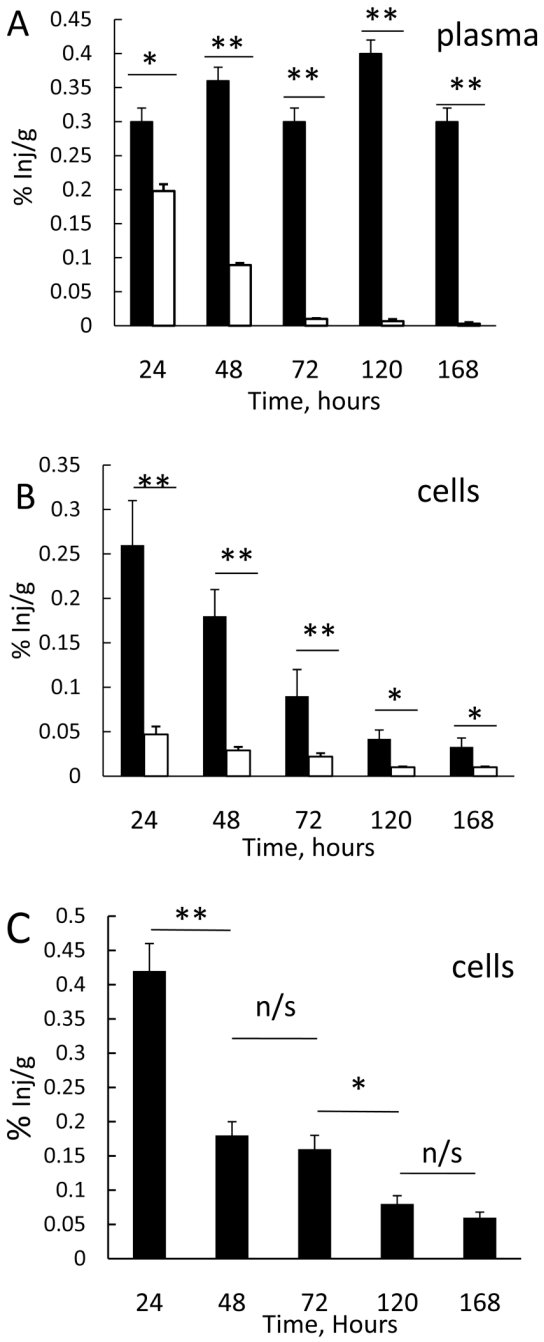

Figure 2. Pharmacokinetic studies demonstrating sustained release of ^{125}I-labeled catalase nanozyme from BMM

Healthy C57Bl/6 mice were injected *i.v.* with ^{125}I-labeled nanozyme loaded into BMM (5×10^6/100µl, 4 µCi/mouse, black bars) or ^{125}I-labelled nanozyme alone (white bars), Figures **A** and **B**. In a parallel experiment mice were injected with ^{125}I-labeled monocytes loaded with non-labeled nanozyme (**Figure C**). Blood samples (100 µl) were taken from facial vein, centrifuged, and radioactivity was recorded in **A**: plasma and **B and C**: cell pellet. Results from N=5 mice per group (± SEM) demonstrating sustained levels of catalase in the plasma of animals injected with nanozyme-BMM and sharp declination of radioactive catalase levels in animals injected with nanozyme alone. The cell fraction of blood samples taken from animals

injected with nanozyme loaded in the BMM showed decrease of radioactive count suggesting that BMM gradually release catalase nanozyme. Decreasing of the amount of radioactively-labeled BMM in the blood indicates that portion of the cells loaded with nanozyme migrate from the blood away into the tissue and then unload and supply the blood plasma with catalase nanozyme from this niche over time. Statistical significance is shown by asterisk *($p<0.05$)*.

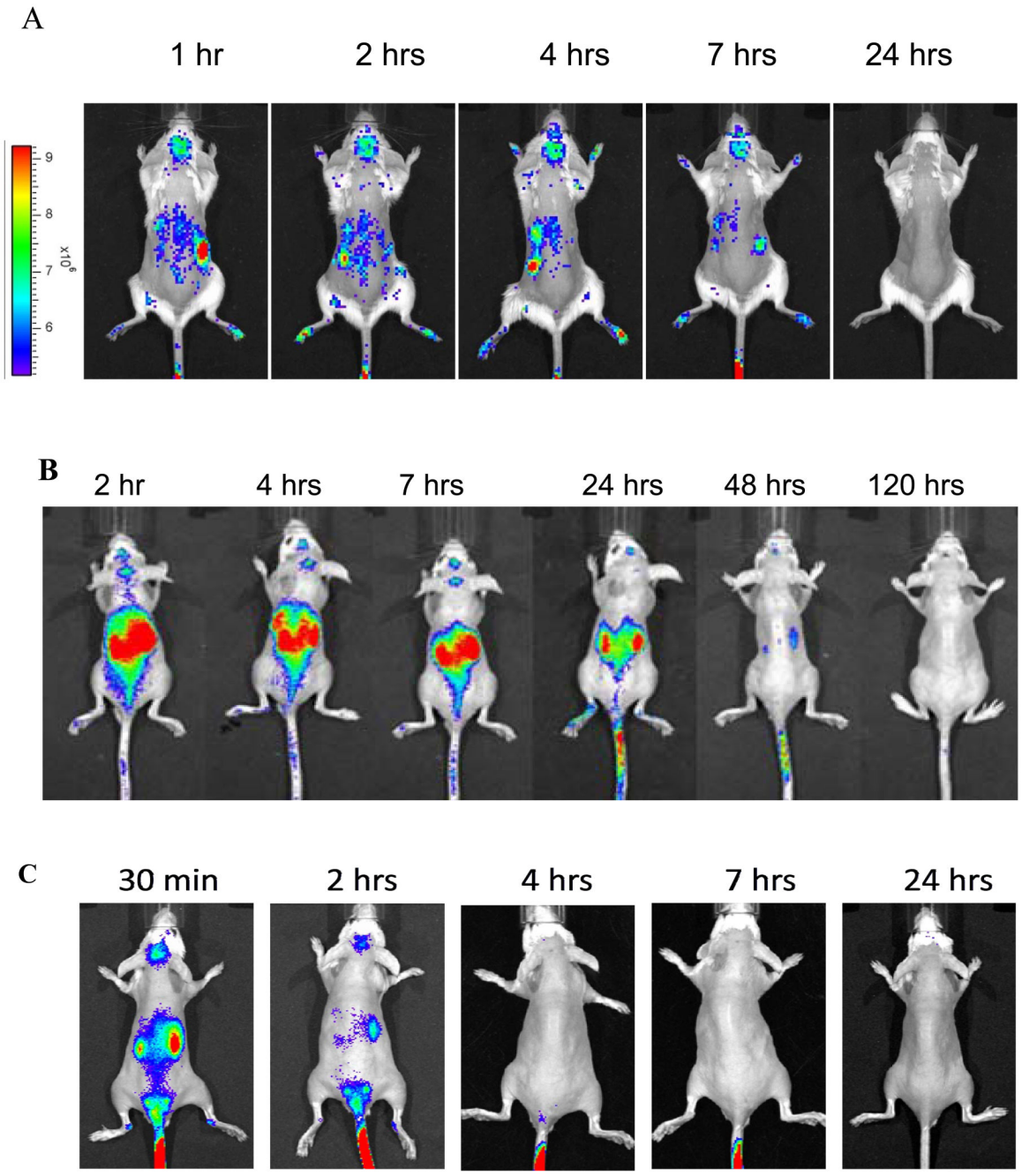

Figure 3. Biodistribution of BMM-carried nanozymes in MPTP-intoxicated mice by IVIS

MPTP-intoxicated Balb/c mice (15 mg/kg) were *i.v.* injected with **A**: Alexa Fluor 680-labeled nanozyme loaded to BMM (5×10^6 cells /mouse); **B**: Alexa Fluor 680-labeled BMM loaded with non-labeled nanozyme, and **C**: Alexa Fluor 680-labeled nanozyme administered alone. Representative images from N=4 mice per group (dorsal planes) taken at various time points demonstrate that both components of the formulation, nanozyme (**A**) and cell carriers (**B**), were detected in the brain area in MPTP-intoxicated animals. Noteworthy, BMM and nanozyme in cell carriers were remained at later time points compared with nanozyme administered alone (**C**).

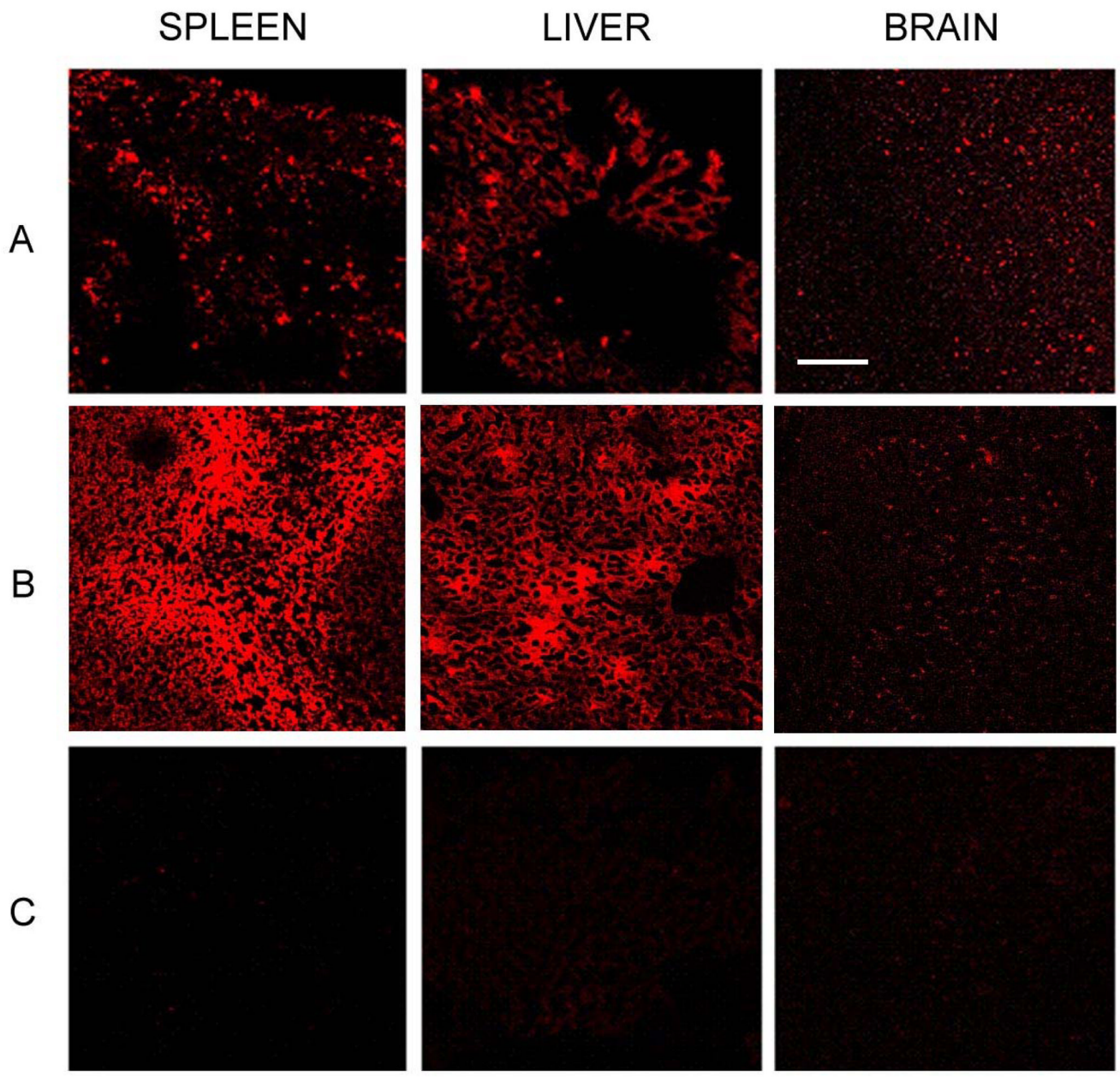

Figure 4. Tracking of BMM loaded with catalase nanozyme in MPTP-intoxicated mice

MPTP-intoxicated C57Bl/6 mice (15 mg/kg) were injected *i.v.* with **A**: rhodamine-labeled BMM (5×10^6 cells/mouse) loaded with non-labeled nanozyme, or **B**: non-labeled BMM loaded with rhodamine-labeled nanozyme, or **C**: PBS. Two hours later mice were sacrificed and perfused with PBS and 4% PFA. Spleen, liver and brain were frozen; tissue specimens were sectioned with a cryostat (10 μm thick) and examined by confocal microscopy (20 × magnification). The bar represents 100 μm. Representative images from N=4 animals demonstrate detectable amounts of BMM in the brain, although, at substantially lower levels than in the liver and spleen.

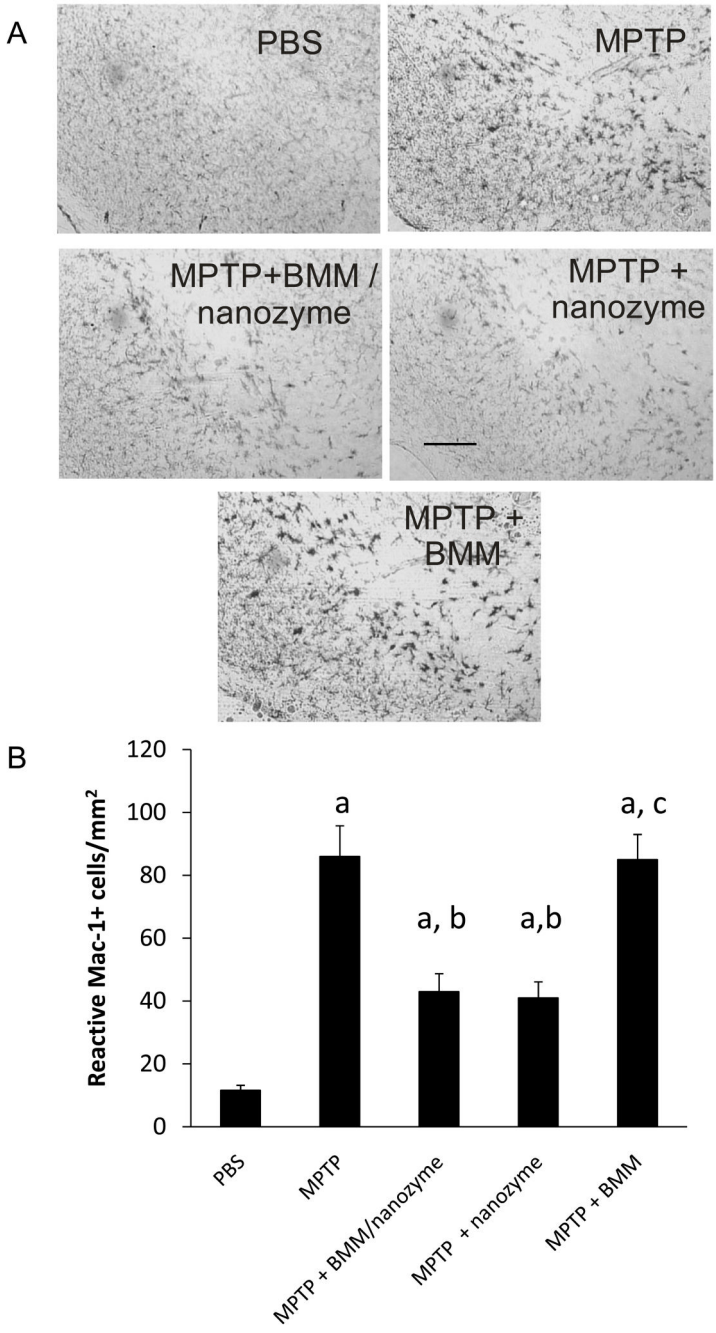

Figure 5. Attenuation of microglial activation in MPTP-intoxicated mice by nanozyme-loaded BMM

MPTP-intoxicated C57Bl/6 mice (18 mg/kg) were injected *i.v.* with PBS (second bar), nanozyme alone (third bar), BMM loaded with nanozyme (5×10^6 cells/mouse/100μl) (fourth bar), or empty BMM (fifth bar). Mice treated with PBS in lieu of MPTP served as non-intoxicated controls (first bar). Forty eight hours later animals were sacrificed, and mid-brain slides were stained for CD11b, a marker for activated microglia. **A**: Representative images of the same experiment (20 × magnification). **B**: Results from N=6 animals per group demonstrating the treatment of MPTP-intoxicated mice with nanozyme-loaded BMM, as well as nanozyme alone, resulted in significantly decreased levels of CD11b compared to non-

treated mice with MPTP intoxication. No effect on microglial activation was detected after treatment with empty BMM. Statistical significance between groups is shown by asterisk *($p<0.05$)* compared with [a]PBS; [b]MPTP; [c]MPTP+BMM/nanozyme. The bar represents 100 μm.

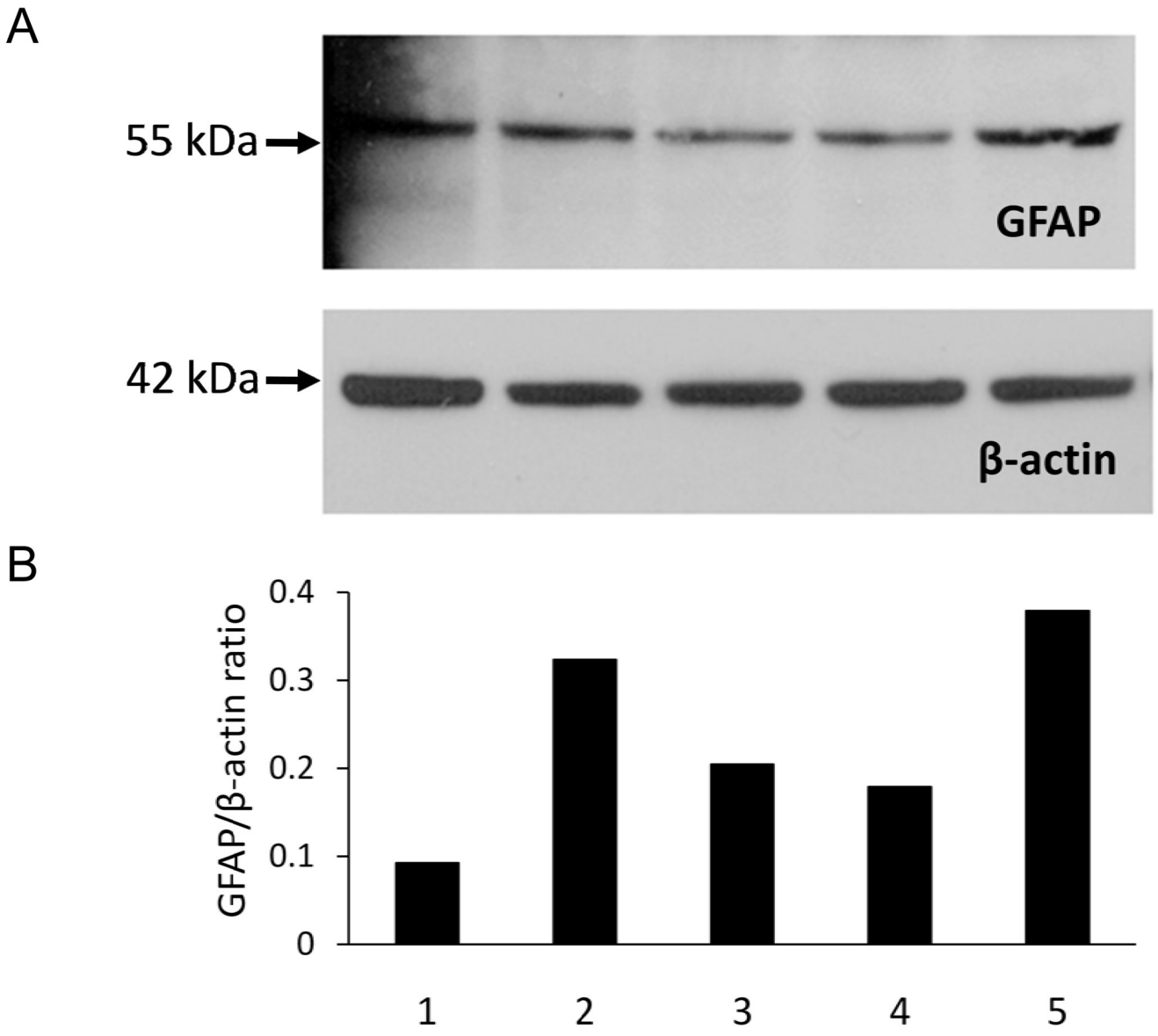

Figure 6. Attenuation of astrocytosis in MPTP-intoxicated mice by nanozyme-loaded BMM

MPTP-intoxicated C57Bl/6 mice (18 mg/kg) were *i.v.* injected with PBS (second bar), nanozyme alone (third bar), BMM loaded with nanozyme (5×10^6 cells/mouse/100μl) (fourth bar), or empty BMM (fifth bar). Mice treated with PBS in lieu of MPTP served as non-intoxicated controls (first bar). Forty-eight hours later animals were sacrificed, and brain tissues were subjected for Western blot with staining for glial fibrillary acidic protein (GFAP). Expression of GFAP shown by **A**: representative gel; and **B**: mean densitometry data. Results from N=6 mice per group demonstrating decrease of neuroinflammation in animals treated with catalase nanozyme loaded into the cells, as well as nanozyme alone. No effect on astrocytosis was detected after treatment with empty BMM.

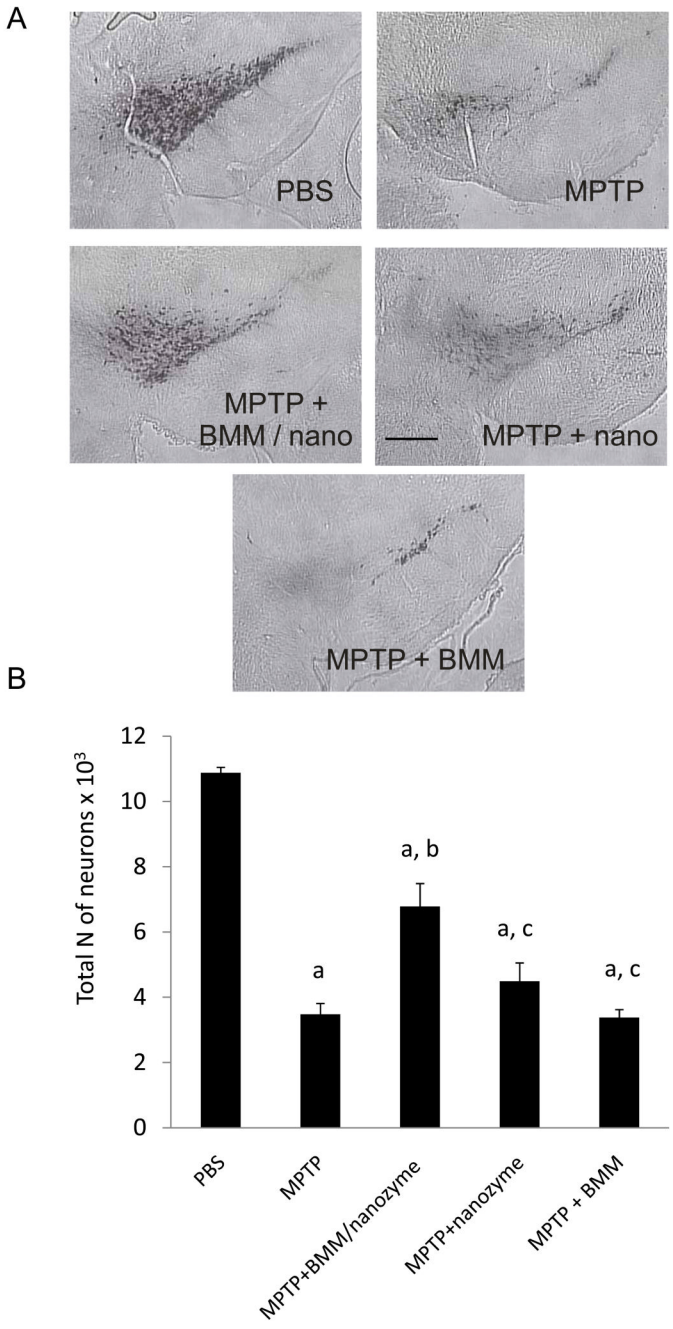

Figure 7. Neuroprotective effect of nanozyme-loaded BMM in an MPTP mouse model of PD

MPTP-intoxicated C57Bl/6 mice (18 mg/kg) were *i.v.* injected with PBS (second bar), nanozyme alone (third bar), BMM loaded with nanozyme (5×10^6 cells/mouse/100μl) (fourth bar), or empty BMM (fifth bar). Healthy non-intoxicated animals were used in a control group (first bar). Seven days later animals were sacrificed, and brain slides were stained for TH-positive nigral dopaminergic neurons. **A**: Representative images of the same experiment. 10 × magnification, bright field microscopy. **B**: Results from N=5 animals per group demonstrating significant loss in MPTP treated mice, which is prevented by adoptive transfer of BMM loaded with nanozyme. No significant neuroprotective effect was detected after

treatment with nanozyme alone, or empty BMM. Statistical significance is shown by asterisk *($p<0.05$)* compared with [a]PBS; [b]MPTP; [c]MPTP+BMM/nanozyme.

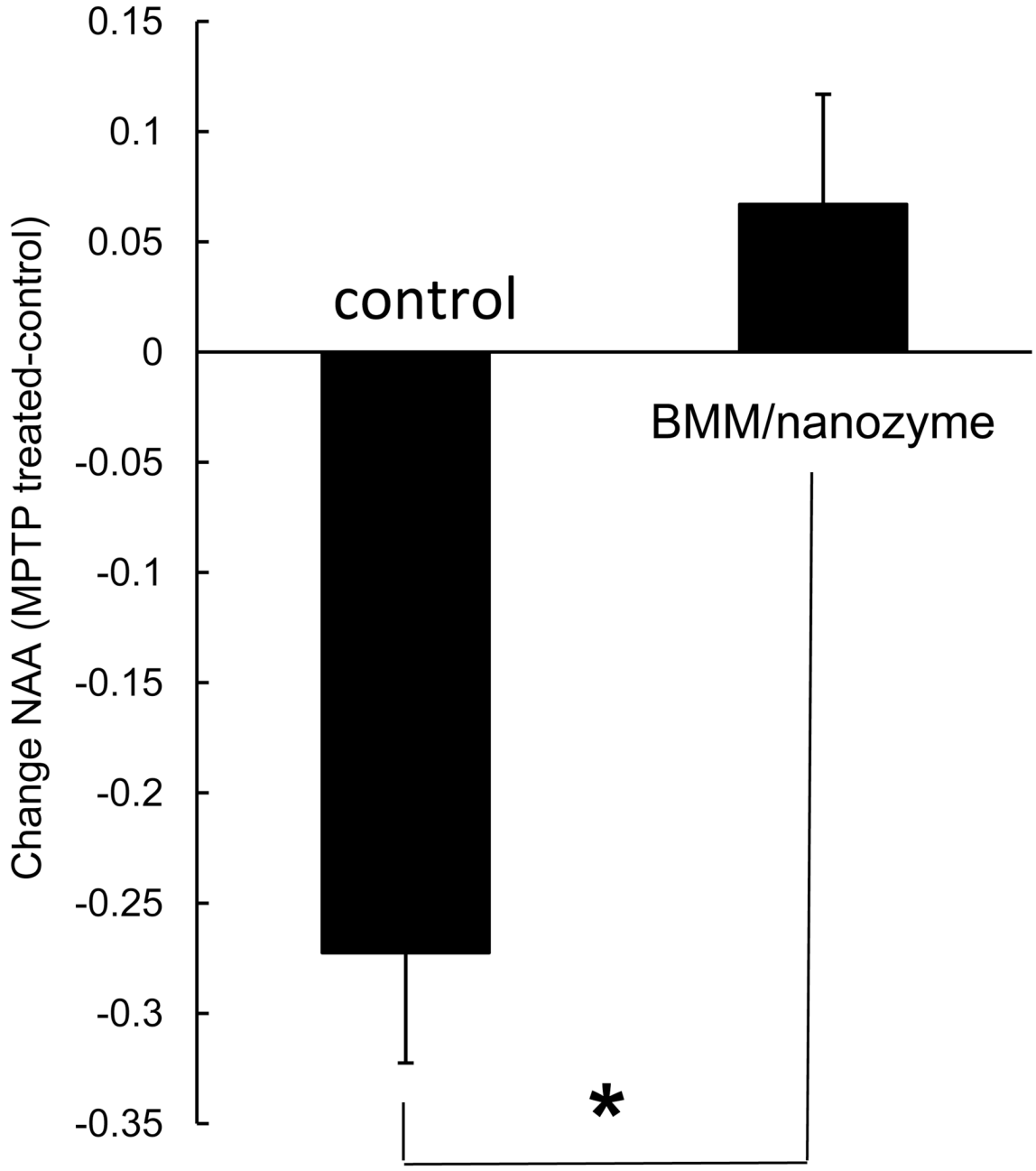

Figure 8. Neuroprotection against MPTP-induced dopaminergic neuronal loss in PD mouse model by ^{1}H MRSI

C57Bl/6 mice were scanned before MPTP treatment (15 mg/kg) and seven days after MPTP intoxications. Control group of MPTP-intoxicated animals (N=4) was injected i.v. with PBS 12 hours after the last MPTP injection. Treatment group of MPTP-intoxicated animals was injected *i.v.* with nanozyme-loaded BMM (5×10^{6} cells/mouse/100μl). Seven days later levels of N-acetylaspartate (NAA) within the SN and striatum were assessed by ^{1}H MRSI in control and treated animals. Differences between readouts (± SEM) of metabolite concentrations of NAA taken seven days after the treatment and before the MPTP treatment were calculated (y-axis). Significant loss of NAA in untreated MPTP-intoxicated mice (left) was prevented in

MPTP-intoxicated mice injected with BMM/nanozyme (right). Statistical significance is shown by asterisk ($p<0.05$)